

# The history of mass assembly of faint red galaxies in 28 galaxy clusters since $z = 1.3$

S. Andreon<sup>★</sup>

*INAF – Osservatorio Astronomico di Brera, via Brera 28, 20121, Milano, Italy*

Accepted 2008 February 12. Received 2008 February 4; in original form 2007 July 18

## ABSTRACT

We measure the relative evolution of the number of bright and faint (as faint as  $0.05L^*$ ) red galaxies in a sample of 28 clusters, out of which 16 are at  $0.50 \leq z \leq 1.27$ , all observed through a pair of filters bracketing the  $4000\text{-}\text{\AA}$  break rest frame. The abundance of red galaxies, relative to bright ones, is constant over all the studied redshift range,  $0 < z < 1.3$ , and rules out a differential evolution between bright and faint red galaxies as large as claimed in some past works. Faint red galaxies are largely assembled and in place at  $z = 1.3$  and their abundance does not depend on cluster mass, parametrized by velocity dispersion or X-ray luminosity. Our analysis, with respect to the previous one, samples a wider redshift range, minimizes systematics and put a more attention to statistical issues, keeping at the same time a large number of clusters.

**Key words:** galaxies: clusters: general – galaxies: evolution – galaxies: formation – galaxies: luminosity function, mass function.

## 1 INTRODUCTION

The evolution of faint red galaxies in clusters is a highly debated topic for two reasons: different observers have claimed controversial results, and clusters of galaxies are often claimed to be interesting laboratories where studying the effect of the environment. Red galaxies, in particular, have different assembly histories in halos of different masses, yet observationally the detection of an environmental dependence of their properties escapes a detection. For example, differences between cluster and field Fundamental Planes are small, if any (Pahre, de Carvalho & Djorgovski 1998), so small that the Coma cluster Fundamental Plane (Jorgensen, Franx & Kjaergaard 1996) is routinely used as zero-redshift reference for studying the evolution of field galaxies, and so small that previous claims of environmental dependencies probably result from having overlooked the difficulty of the statistical analysis (van Dokkum & van der Marel 2007). Similarly, the colour of the red sequence seems not to depend on cluster-centric distance (Pimbblet et al. 2002; Andreon 2003) or galaxy number density (Hogg et al. 2004; Cool et al. 2006).

The red colour, by which red galaxies are defined and selected, induces a selection effect: at every redshift only galaxies whose stellar populations are red (i.e. old, modulo dust, of no interest here) enter the sample. It is not a surprise then to find old selected populations to be old. A different question is whether galaxies that have an old stellar population were fully assembled at early or late times. Answering this question requires a measurement of the abundance of red galaxies as a function of look-back time. For clusters, there

is a further complication: clusters have different richnesses, jeopardizing any look-back time trend if the richness dependence is not factored out. It is easy, furthermore, to qualitatively claim that the red sequence is built later (i.e. a lower redshift) in poor environments than it is in dense environments, but this might just be do to signal to noise issues, because in poorer environments the red population is a minority one, and its contrast with respect to other populations (e.g. background) noisier. A sound statistical assessment of the abundance of faint red galaxies is therefore compelling.

Usually, the richness dependence of the abundance of faint red galaxies is removed by normalizing it to the number of bright red galaxies, that is, by computing the faint-to-luminous ratio, or any related quantity, like the faint-end slope  $\alpha$  of the luminosity function (LF). The analysis of the faint-to-luminous ratio, performed by Stott et al. (2007), or its reciprocal, the luminous-to-faint ratio by De Lucia et al. (2007), both suggest an evolution of the relative abundance of faint red galaxies, in the sense that at high redshift there is a deficit of faint red galaxies per unit bright galaxy. On the other end, Andreon (2006a) suggests no deficit of red galaxies, using a very small cluster sample, and Andreon et al. (2006) discard a considerable build-up of the red sequence on the basis of fossil evidence. Evidences presented in earlier works have been discussed in the mentioned papers and references therein.

In this paper, we aim to understand if the colour–magnitude relation has been built up at early or late times, by studying many galaxy clusters at several look-back times.

Throughout this paper, we assume  $\Omega_M = 0.3$ ,  $\Omega_\Lambda = 0.7$  and  $H_0 = 70 \text{ km s}^{-1} \text{ Mpc}^{-1}$ . All results of our stochastical computations are quoted in the form  $x \pm \sigma$ , where  $x$  is the posterior mean and  $\sigma$  is the posterior standard deviation.

<sup>★</sup>E-mail: stefano.andreon@brera.inaf.it

## 2 DATA AND DATA REDUCTION

This work makes use of archive data. The selection criteria used for the inclusion in our sample are the following. (i) All observations must include a pair of filters bracketing the 4000-Å break in the cluster rest frame. (ii) Control field observations with identical conditions (same telescope, instrument, filters, depth and seeing) as cluster observations must be available. (iii) Observations had to be deep enough to measure the faint-end slope of the LF. (iv) Clusters had to be spectroscopically confirmed. (v) Data should be publicly available at the start of this work.

Our sample is formed by the following three sets. (i) 15 high-redshift clusters observed with the Wide Field Camera of the Advanced Camera for Surveys (hereafter ACS, Ford et al. 1998, 2003) of *Hubble Space Telescope (HST)*. (ii) Two low-redshift clusters observed by the Sloan Digital Sky Survey (SDSS). (iii) Two LFs from the literature, one for a  $z \sim 0.25$  cluster sample and one for one more high redshift cluster observed by *HST* but with the Wide Field Planetary Camera 2.

Table 1 lists the ACS sample, formed by 15 clusters at  $0.5 \leq z \leq 1.27$ . More than 150 *HST* orbits, devoted to clusters, have been reduced and analysed for this paper. As we need to statistically discriminate against fore- and back-ground interlopers, Table 1 also lists the adopted control fields. A control field matching the filter pair used for clusters is available for all targets.

In order to provide a local ( $z \sim 0$ ) reference, we use SDSS  $u$ ,  $g$  data of two nearby clusters: Abell 1656 (A1656, i.e. Coma,  $z = 0.023$ ) and Abell 2199 (A2199,  $z = 0.030$ ). Given the large SDSS sky coverage, the control field for our nearby clusters is taken all around them.

Finally, the LF of 10  $z \sim 0.25$  clusters, observed in  $B$  and  $I$  filters by Smail et al. (1998), and of MS1054 at  $z \sim 0.8$ , observed with the *HST* Wide Field Planetary Camera 2 in  $F606W$  and  $F814W$  and presented in Andreon (2006) have been taken from the literature. These LFs are fully homogeneous to those computed in this work.

**Table 1.** The ACS  $z \geq 0.5$  cluster and control field samples.

Name	$z$	$N^1$	Filters	
			Blue	Red
Lynx W	1.27	3	<i>F775W</i>	<i>F850LP</i>
Lynx E	1.26	3	<i>F775W</i>	<i>F850LP</i>
RDCS J1252–2927	1.23	4	<i>F775W</i>	<i>F850LP</i>
RDCS J0910+5422	1.11	1	<i>F775W</i>	<i>F850LP</i>
GHO 1602+4329	0.92	1	<i>F606W</i>	<i>F814W</i>
GHO 1602+4312	0.90	1	<i>F606W</i>	<i>F814W</i>
1WGA J1226.9+3332	0.89	6	<i>F606W</i>	<i>F814W</i>
MACS J0744.8+3927	0.70	1	<i>F555W</i>	<i>F814W</i>
MACS J2129.4–0741	0.59	1	<i>F555W</i>	<i>F814W</i>
MACS J0717.5+3745	0.55	1	<i>F555W</i>	<i>F814W</i>
MACS J1423.8+2404	0.54	1	<i>F555W</i>	<i>F814W</i>
MACS J1149.5+2223	0.54	1	<i>F555W</i>	<i>F814W</i>
MACS J0911.2+1746	0.50	1	<i>F555W</i>	<i>F814W</i>
MACS J2214.9–1359	0.50	1	<i>F555W</i>	<i>F814W</i>
MACS J0257.1–2325	0.50	1	<i>F555W</i>	<i>F814W</i>
CT344		1	<i>F606W</i>	<i>F814W</i>
B0455		1	<i>F555W</i>	<i>F814W</i>
GOODS + PAN		$\sim 30$	<i>F775W</i>	<i>F850LP</i>

<sup>1</sup>Number of ACS field of view per filter.

All clusters have coordinates and redshifts listed in NED, except for MACS clusters, listed in Ebeling et al. (2007). MACS clusters have been also studied by Stott et al. (2007).

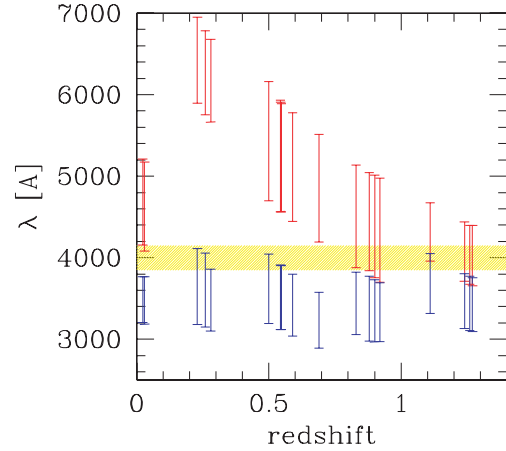


**Figure 1.** Rest-frame  $\lambda$  sampling of the adopted filters for the clusters studied in this work. The shaded (yellow) band marks the 4000-Å break. All clusters have been observed in a pair of filters bracketing the 4000-Å break. The sample is formed by 28 clusters, some of which have very similar redshifts and do not show up individually in the figure.

Fig. 1 shows that all clusters have a pair of filters bracketing the 4000-Å break.

The raw ACS data listed in Table 1 were processed through the standard CALACS pipeline (Hack 1999) at STScI. This includes over-scan, bias, and dark subtraction, as well as flat-fielding. Image combination has been done with the MULTIDRIZZLE software (Koekemoer et al. 2002). The data quality arrays enable masking of known hot pixels and bad columns, while cosmic rays and other anomalies are rejected through the iterative drizzle/blot technique. Sources are detected using SExtractor (Bertin & Arnouts 1996), making use of weight maps produced by MULTIDRIZZLE. Star/galaxy separation is performed by using the stellarity index given by SExtractor. *HST* images are calibrated in the Vega system, using the zero points provided in the *HST* data handbook. Completeness is computed as in Garilli, Maccagni & Andreon (1999), from the brightest luminosity of the detected objects of faintest surface brightness. Only data brighter than the completeness magnitude are kept.

All science (i.e. cluster) and two of the control fields, CT344 and BO0455, have been combined (and catalog built) by myself, while the remaining control field, GOODS+PAN, has been generously given to us by D. Macchetto. These images come from the same telescope, instrument and filters and have been processed with the same software as science data (i.e. CALACS, MULTIDRIZZLE and SExtractor), but have been combined by someone else (than the author). By reducing by myself part of the GOODS+PAN data, we checked that their and our reductions are indistinguishable.

The left panel of Fig. 2 shows galaxy counts of red galaxies, where ‘red’ is taken to mimic our later selection, for two widely different sky directions: CT344 and a field in Benitez et al. (2004). The right panel shows the colour distribution in the two directions. Differences between the two sky directions are comparable to Poisson errors on the average value. Therefore, for areas, magnitudes and colours of interest in this paper, non-Poisson fluctuations of galaxy counts can be neglected.

For the nearby cluster sample, catalogs have been extracted from the SDSS 5th data release (Adelman-McCarthy et al. 2007), which have been produced by the SDSS pipeline and are not calibrated in the Vega system. We checked that synthetic  $U$ ,  $V$  and  $U - V$  computed from  $u$ ,  $g$  SDSS photometry is indistinguishable from

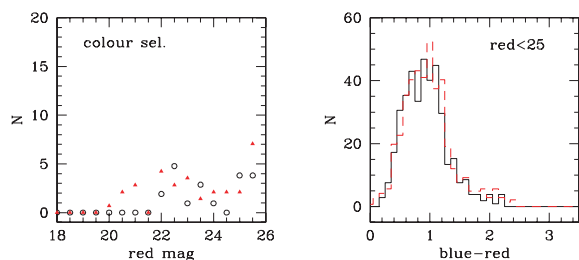


**Figure 2.** Minor role of non-Poisson variance. The left-hand panel shows galaxy counts of red galaxies in two widely different sky direction, whereas the right-hand panel shows their colour distribution. Differences between sky directions are within Poisson fluctuations.

observed  $U$ ,  $V$  and  $U - V$  photometry for red galaxies in the A1656 cluster direction, taken from Terlevich, Caldwell & Bower (2001), and derived with traditional techniques (stare exposures, calibration in the Vega system, and catalogs built with SExtractor).

### 3 FAINT-TO-LUMINOUS RATIO OF RED GALAXIES

We modelled the distribution of galaxies in the red sequence as Gauss-distributed in colour at every magnitude and Schechter (1976) distributed in magnitude. The mean colour of the Gauss varies linearly with magnitude, because the color-magnitude relation is linear. Furthermore, we allow a broadening of the colour-magnitude relation due to both photometric errors and an intrinsic scatter. As explained in appendix A in Andreon (2006a), with Bayesian methods we solved at once for all parameters (colour-magnitude slope, intercept and intrinsic scatter, characteristic magnitude  $M^*$ , faint-end slope  $\alpha$ , and normalization of the Schechter, background parameters), hence fully accounting for the background (including uncertainty, variance and covariance with all parameters).

Our definition of red is ‘galaxies under the Gauss centred on the red sequence’, similar to some SDSS works (e.g. Balogh et al. 2004; Ball et al. 2006). Previous studies (Andreon et al. 2006; De Lucia et al. 2007) have shown that the precise definition of ‘red’ has a negligible impact on the results. We have checked it for our own

**Table 2.** Extraction radius  $r$  in arcmin, faint-end slopes  $\alpha$  and luminous-to-faint ratios  $L/F$ s.

Cluster name	$r$	$\alpha$	$L/F$
Lynx E + W	1.0	$-1.12 \pm 0.22$	$0.57 \pm 0.15$
RDCS J1252–2927	1.0	$-0.89 \pm 0.37$	$0.57 \pm 0.16$
RDCS J0910+5422	1.0	$-0.77 \pm 0.36$	$0.60 \pm 0.14$
GHO 1602+4329	1.0	$-0.54 \pm 0.38$	$1.03 \pm 0.42$
GHO 1602+4312	1.0	$-0.67 \pm 0.33$	$0.84 \pm 0.23$
1WGA J1226.9+3332 (CL1226)	1.5	$-0.97 \pm 0.33$	$0.29 \pm 0.07$
MACS J0744.8+3927	1.4	$-0.34 \pm 0.31$	$0.67 \pm 0.12$
MACS J2129.4–0741	1.4	$-0.78 \pm 0.18$	$0.52 \pm 0.08$
MACS J0717.5+3745	1.4	$-1.04 \pm 0.07$	$0.72 \pm 0.06$
MACS J1423.8+2404	1.3	$-0.89 \pm 0.16$	$0.74 \pm 0.14$
MACS J1149.5+2223	1.2	$-0.92 \pm 0.09$	$0.65 \pm 0.07$
MACS J0911.2+1746	1.2	$-0.78 \pm 0.16$	$0.53 \pm 0.08$
MACS J2214.9–1359	1.3	$-0.76 \pm 0.12$	$0.71 \pm 0.09$
MACS J0257.1–2325	1.3	$+0.02 \pm 0.31$	$0.35 \pm 0.07$
A2199	48.0	$-1.12 \pm 0.06$	$0.48 \pm 0.04$
A1656	48.0	$-1.02 \pm 0.05$	$0.44 \pm 0.04$

sample and our definition, by adopting a simpler definition of red (within  $2\sigma$  from the red sequence, plotted as dots in Fig. 3).

The luminous-to-faint ratio is computed as the ratio of the number of galaxies on the red sequence in appropriate absolute magnitude ranges. The number of galaxies in a given range is, by definition, the integral of the LF over the concerned range. The range definitions are taken from De Lucia et al. (2007):  $M_V < -20$  mag and  $-20 < M_V < -18.2$  mag. Magnitudes are passively evolving, modelled with a simple stellar population of solar metallicity, Salpeter initial mass function, from Bruzual & Charlot (2003), as in De Lucia et al. (2007). As a sanity check, the same model has been checked to reproduce the colour of the red sequence at  $M_V = -20.0$  mag for all our clusters.

From now on, the two Lynx clusters are stacked together to improve the signal to noise. LFs are computed for galaxies within a cluster-centric radius listed in Table 2. The considered region has been chosen as a compromise between sampling a large portion of the cluster and not including a too large contribution from background galaxies. MACS clusters are larger than the instrument field

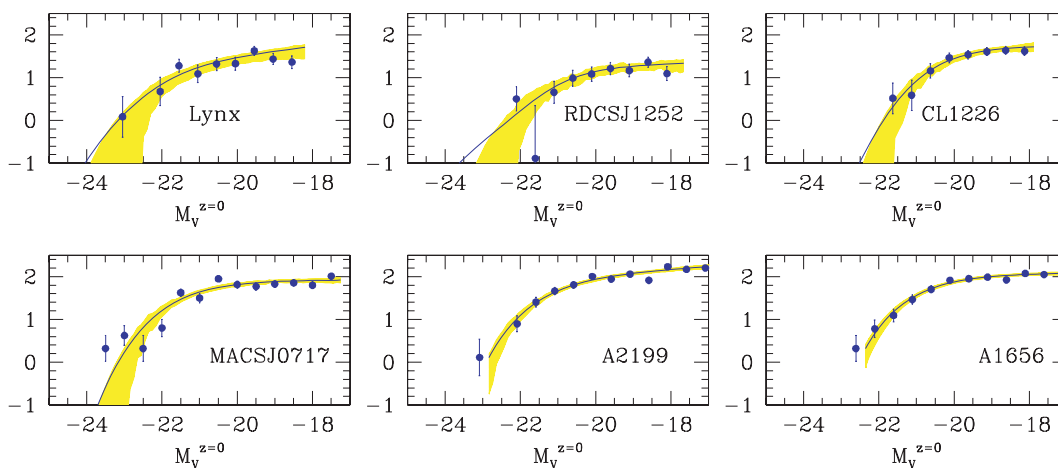


**Figure 3.** Luminosity function of red galaxies in some (to save space) of our clusters. The solid curve and the shaded region mark the LFs and its (highest posterior) 68 per cent error region as computed with Bayesian methods. Points and error bars mark simply derived LFs, computed as difference of counts in the cluster and reference lines of sight, using ‘within  $2\sigma$  from the colour-magnitude relation’ as definition of red. The top left-hand panel refers to the two Lynx clusters stacked together.

of view, and therefore we choose the largest radius that fit in the fully exposed part of the image, consistently with the choices of Andreon (2006a) and Smail et al. (1998), whose LFs are included in this work, as mentioned.

The potential dependency of the LF slope on the considered cluster portion has a small impact on our study, because we explicitly allows the observed value of the slope to scatter around to its true value by more than its uncertainty. In fact, in the next section we we allow an intrinsic scatter in our model: see equation (1). This argument is developed further in Section 4.2.

#### 4 RESULTS

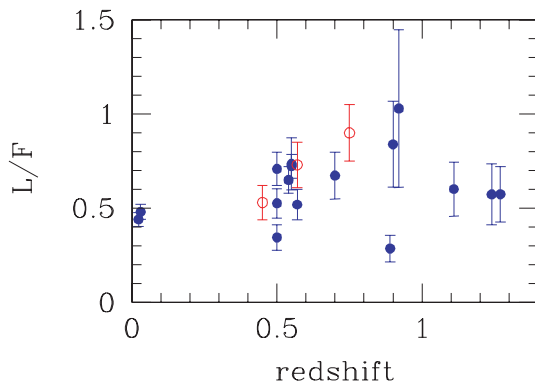
Fig. 3 shows the LF of a subset (to save space) of studied clusters.

Fig. 4 shows the luminous-to-faint ratio,  $L/F$ , as a function of redshift for clusters with LFs measured in this paper (solid points). Our data are in agreement with De Lucia et al. (2007) data (open points), but our wider redshift coverage suggests a shallower trend than the one hinted in De Lucia et al. (2007) from their data points.

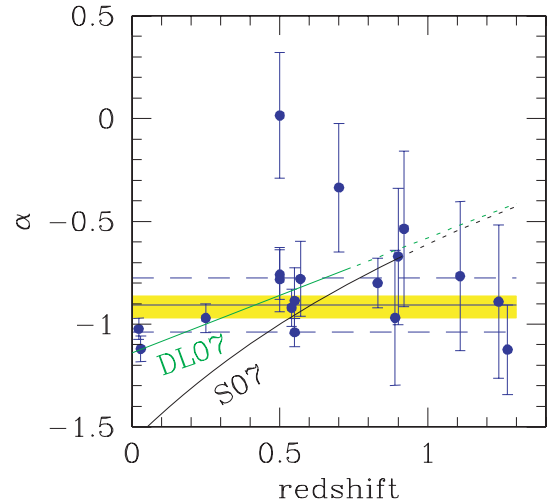
In this work we refrain to perform inferences using  $L/F$  or its reciprocal,  $F/L$ , for reasons detailed in sec 4.4, mainly of statistical nature. The use of the faint end slope,  $\alpha$ , is a measure of the faint-to-luminous ratio, it is easier to deal with from a statistical point of view, and has the further advantage that it uses all the data available, including data fainter than  $-18.2$  mag that would be otherwise wasted using  $L/F$ .

Fig. 5 shows the slope,  $\alpha$ , as a function of redshift for the whole cluster sample, that is, for 28 clusters, of which 16 at  $z \geq 0.5$ . Marginalization accounts for the known correlation between parameters (e.g.  $M^*$  and  $\alpha$ ). For example, the large error of some data points is due to the fact that many ( $M^*$ ,  $\alpha$ ) pairs fit almost equally well the data and thus a large range of  $\alpha$  values is acceptable.  $\alpha$  errors also account for differences in the galaxy background counts in the cluster and control field lines of sight, because, as mentioned, we ‘solve’ for all parameters at once (technically, we marginalize over other parameters). Table 2 lists the  $\alpha$  and  $L/F$  values found.

The data are in agreement with the lack of a deficit of faint red galaxies suggested by Andreon (2006a) on the basis of a very small sample of clusters and reject some trends suggested in previous



**Figure 4.** Relative abundance of faint and bright red galaxies, as parametrized by the luminous-to-faint ratio, for clusters with LFs measured in this paper (solid dots) and in (open points De Lucia et al. 2007). Although in agreement, our data indicate a shallower trend with redshift than that indicated by De Lucia et al. (2007) data points. Two points at  $z = 0.55$  fall one on the top of the other.



**Figure 5.** Relative abundance of faint and bright red galaxies, as parametrized by the faint slope  $\alpha$  of the cluster LF for the whole sample of 28 clusters studied here. The redshift dependence of the relative abundance of bright red galaxies is small, if any. The point at  $z = 0.25$  ( $z = 1.27$ ) is the average of 10 (2) clusters. The shaded (yellow) region shows the (highest posterior density) 68 per cent error region. The dashed lines delimit the  $\pm 1\sigma$  intrinsic (i.e. not accounted for measurement error) scatter. The trends proposed by Stott et al. (2007) and fitted on De Lucia et al. (2007) data are also marked with the solid lines (labelled by ‘S07’ and ‘DL07’, respectively) up the largest studied redshift by them, and marked with the dotted lines afterwards.

works. Let us consider: (i) our maximum-likelihood fit of the  $L/F$  data points in fig. 9 of De Lucia et al. (2007) and (ii) the Stott et al. (2007)  $F/L$  versus  $z$  fit. The two fits have been transformed in  $\alpha$  versus  $z$  trends using the  $L/F$ ,  $F/L$  and  $\alpha$  definitions. Fig. 5 shows that at low and intermediate redshift the De Lucia et al. (2007) trend, marked with ‘DL07’, is compatible with our data. However, a constant, that is, a more economical model having one degree of freedom less, also well describes our data (and also theirs, see Fig. 5) over the common redshift range ( $z < 0.8$ ) and, actually, also above. Furthermore, neither De Lucia et al. (2007) nor our data request a more complex model than a constant plus an intrinsic scatter. The computation of the Bayes factor shows that the De Lucia et al. (2007) trend is disfavored, with respect to ‘no trend at all’ by our data with odds 14:1, that is, there is moderate evidence against an increase of the luminous-to-faint ratio as large as pointed out by De Lucia et al. (2007). We refrain, therefore, from fitting a more complex model, and we adopt a constant model. Fig. 5 also shows that the Stott et al. (2007) fit, marked with ‘S07’ in the figure, nicely reproduces the observed values in the reduced redshift range,  $0.5 \leq z \leq 0.6$ , where we share clusters and *HST* data with them, but disagrees outside it, in particular at low redshifts. Furthermore, in the local universe, the Stott et al. (2007) fit and data also disagree with De Lucia et al. (2007) data and trend. Our data clearly discard the trend proposed by Stott et al. (2007).

Using Bayesian methods (D’Agostini 2003, 2005) and uniform priors, we ‘fitted’ the data point with a constant, accounting for errors and allowing an intrinsic (i.e. not accounted for errors) Gaussian scatter,  $\mathcal{N}(0, \sigma_{\text{intr}})$ . We found

$$\alpha(z) = -0.91 \pm 0.06 + \mathcal{N}(0, 0.13 \pm 0.06) \quad (1)$$

displayed in Fig. 5. Using our own data alone, that is, ignoring the Smail et al. (1998)  $z = 0.25$  composite cluster, we found an

indistinguishable result

$$\alpha(z) = -0.89 \pm 0.06 + \mathcal{N}(0, 0.16 \pm 0.06). \quad (2)$$

#### 4.1 Richness dependency

Koyama et al. (2007), on the basis of three clusters at  $z \sim 0.8$ , suggested that the relative abundance of faint red galaxies is dependent on cluster richness or mass (actually, X-ray luminosity in their work), in the sense that poorer systems show stronger deficits. Figs 6 and 7 plot two deficit estimators, the slope  $\alpha$  and the  $L/F$  ratio, versus two mass estimators, X-ray luminosity and velocity dispersion, for clusters at  $z \geq 0.5$ . X-ray luminosities are taken from Ettori et al. (2004), Lubin, Mulchaey & Postman (2004) and Ebeling et al. (2007). They come from *Chandra*- or *XMM*-pointed observations and have, typically, errors of 10 per cent or less. MACS luminosities, in the 0.1–2.4 keV band are converted in bolometric assuming a thermal bremsstrahlung spectrum with the measured temperature. Velocity dispersions are taken from Ebeling et al. (2007), Stanford et al. (2001) and Maughan et al. (2004). The solid dots emphasize clusters in the reduced redshift range  $0.50 \leq z \leq 0.70$ , to limit the (negligible, see previous section) effect of evolution. There is no obvious trend between cluster mass and the relative abundance of faint red galaxies. The (green) crosses, we connected by a solid line in the top panel of Fig. 6, show the three clusters studied by Koyama et al. (2007), one of which is MS1054.4–0321, the latter taken from

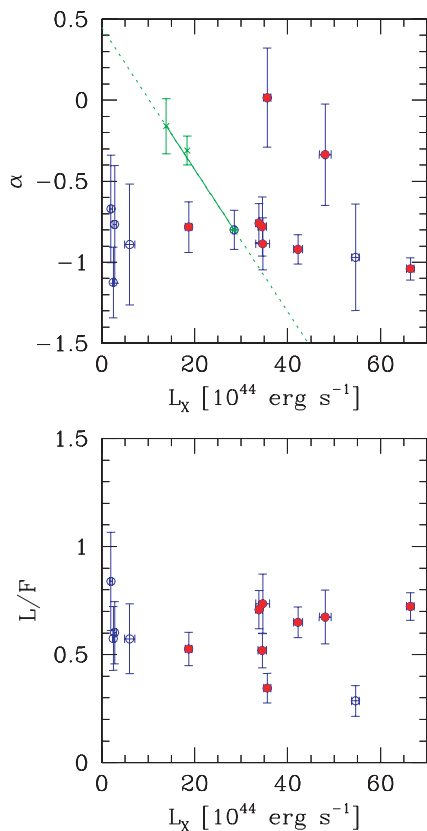


**Figure 6.** Cluster mass dependency, as parametrized by X-ray bolometric luminosity, of the relative abundance of faint red galaxies, as parametrized by the  $\alpha$  (top panel) or the luminous-to-faint ratio (bottom panel), for clusters with  $z \geq 0.5$ . Clusters in the  $0.5 \leq z \leq 0.70$  range are marked with a solid (red) dot. The three crosses connected by a solid line in top panel mark clusters used by Koyama et al. (2007) to suggest a mass-dependent trend in the relative abundance of faint red galaxies.

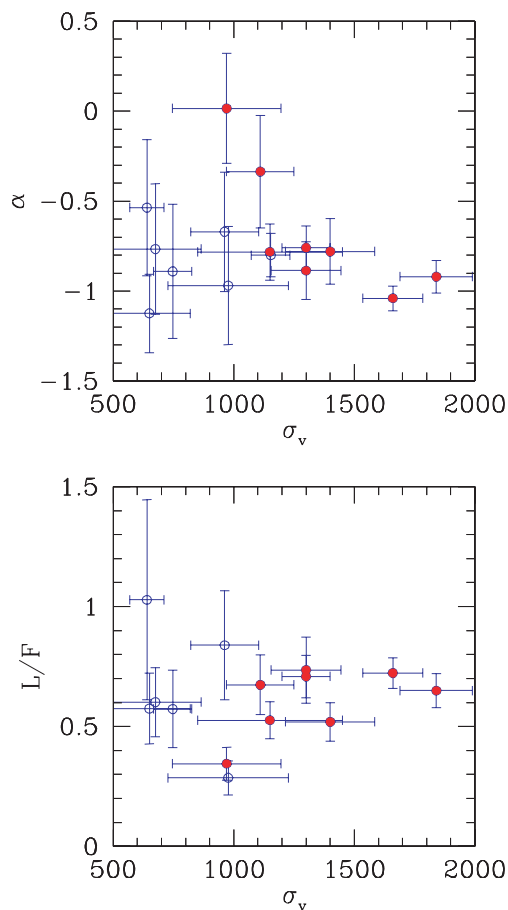


**Figure 7.** The same as Fig. 6, but using velocity dispersion as cluster mass estimator.

Andreon (2006a). The slope  $\alpha$  is derived by us from their luminous over faint ratio assuming a Schechter function. The figure shows that the observed slopes  $\alpha$  are plausible, since two other clusters in our sample show similar values of the relative abundance of faint red galaxies. However, the trend suggested by these three points (slanted line) is clearly too steep, and obviously ruled out by our data. Finally, we note that RX J0152.7–1357 point, that is, the middle point of the three plotted, has been put in Koyama et al. (2007) and in our plot at the *sum* luminosity of the two subclumps that form the cluster, not at the *mean*  $L/F$  value. Would the RX J0152.7–1357 point be put at the average X-ray luminosity of the two clumps, the one typically experienced by galaxies in this clusters and consistently with the choice of quoting a mean  $L/F$ , the three  $L/F$  points would no longer show any monotonic trend with X-ray luminosity.

In conclusion, the abundance of faint red galaxies does not considerably depend on cluster mass (in the range sampled by data, of course) with the Koyama et al. (2007) trend largely based on a sample of inadequate size, given the large intrinsic scatter, a possibility also mentioned by these authors.

#### 4.2 Radius- and scatter-related effects and the advantages of allowing an intrinsic scatter

Clusters have no sharp boundaries. In order to understand the potential effect of the choice of the studied cluster portion, we compute  $\alpha$  and  $L/F$  of A1656 cluster within two cluster-centric radii:  $0:2$  and  $0:8$ . A1656 cluster has been chosen because it has the best deter-

mined values of  $\alpha$  and  $L/F$  among all our clusters. For A1656, the relative abundance of faint red galaxies, as parametrized by these quantities, is the same within the two radii. Although this test is reassuring, we cannot generalize from a single example.

Our model, equation (1), explicitly allows an intrinsic variance in the relative abundance of faint red galaxies, due for example to the mentioned cluster-centric dependence, cluster-to-cluster or other possible (unknown, for the time being) systematics. These terms are thus a source of scatter, not different from a random number added to each measurement. We model such random process, whatever its physical nature is related to cluster-centric distance, to cluster-to-cluster variance or whatsoever unidentified reason, with a normal (Gaussian) of unknown variance (equation 1), for lack of evidence towards any more complex model. In passing, in absence of more information, the Gaussian is the maximum entropy choice among all real-valued distributions with specified mean and standard deviation (e.g. Sivian 2006). The sum rule of probability states that in order to proceed with the inference, we need to marginalize over this (nuisance) parameter. The intrinsic scatter parameter, and its consequent marginalization, offers protection against claiming a trend when just too few data are available: marginalization spreads the probability of a (redshift or mass) trend over a large range of slope values, that is, quantifies the researcher good sense that when just a few data points are available and an intrinsic scatter is there, one should be prudent in claiming the existence of a trend. Assuming a single value for the intrinsic scatter, as other authors sometime implicitly take when looking for a trend, artificially collapses the error ellipse along this axis and leads to determinations with overly optimistic confidence.

Therefore, since the model allows an intrinsic scatter, the analysis of the redshift dependence of the relative abundance of faint red galaxies is correct even if: (i) a cluster-centric dependence of the the relative abundance of faint red galaxies exists, provided that we are not sampling increasing smaller cluster portions as the redshift increases or decreases, or (ii) the relative abundance of faint red galaxies differs from cluster to cluster. Both cases are just source of scatter and our model account for them.

As mentioned, we found a non-zero intrinsic (i.e. not accounted for measurement errors) scatter ( $\sigma_{\text{intr}} = 0.13 \pm 0.06$ ), quantifying past claims of a heterogeneity in the relative abundance of faint red galaxies. An inspection of the colour–magnitude relations of outliers in Fig. 5, for example, MACS J0257.1–2325, confirms that these clusters have an underpopulated red sequence at faint magnitude or an overpopulated one at bright ones.

Therefore, in the quest of a build-up of the red sequence, an intrinsic scatter must be allowed, in order not to overweight ‘outlier’ clusters, and not to overstate the precision and the statistical significance of the found (redshift, mass or whatever) trend. We note that the existence of an intrinsic scatter has been claimed in previous works (De Lucia et al. 2007; Stott et al. 2007) but ignored (Stott et al. 2007) or not rigorously accounted for (De Lucia et al. 2007) when establishing the veracity of the claimed redshift trend.

The existence of an intrinsic scatter testifies that: (i) there is a yet to be identified physical mechanism that affects the relative abundance of faint red galaxies, and (ii) present data are of adequate quality to perform such measurement, that is, the topic deserves further investigation.

### 4.3 Joining high- and low-redshift information

We emphasize that our (past) knowledge about individual nearby clusters tell us that at least some galaxies on the red sequence have

a spiral morphology (Butcher & Oemler 1984; Oemler 1992; see fig. 3a in Andreon 1996 or fig. 4 in Terlevich et al. 2001 for A1656 galaxies). Their spiral arms testify that, in the past, these galaxies were forming stars, that is, were blue, and therefore were not on the red sequence. Furthermore, at least for A1656 (Coma), red spirals have lower surface brightness than blue spirals (Andreon 1996), as expected if the former are the descendents of the latter. Since, on average, spirals are fainter than early-type galaxies (e.g. Binggeli, Sandage & Tammann 1988 for Virgo, Andreon 1996 for A1656), we expect that the abundance of faint red galaxies grows somewhat with time, just because of the evolving colour (towards the red) of some spirals. However, it cannot grow too much, otherwise it would bend the colour–magnitude and inflate its scatter. The argument is the usual one (e.g. Bower, Lucey & Ellis 1992): (i) a heterogeneity in the star formation history leads to a heterogeneous population in colour (unless something else coordinately conspires to keep the colour scatter small); and (ii) a delayed stop of the last star formation episode delays the arrival of a galaxy on the colour–magnitude relation, bending it (or increasing the colour scatter if there is an un-delayed population). In Abell 1185 the colour–magnitude relation is linear and the scatter in colour is small (0.04 mag) down to  $M^* + 8$  (Andreon et al. 2006). In A1656, the scatter stays constant to low levels (0.05 mag) down to  $M^* + 4$  (Eisenhardt et al. 2007). Therefore, fossil evidence points towards a small, but not null, differential build-up of red sequence galaxies.

Theory (De Lucia et al. 2007) shows that a model in which star formation histories of blue galaxies are truncated produces an important change in the luminous-to-faint ratio, larger than allowed by De Lucia et al. (2007) data, producing too many faint galaxies by a factor two (but note that these authors consider it as ‘approximately consistent’ with their data). Direct measurement of the abundance of red faint galaxies over redshift (this paper) indicates a shallower trend with redshift than suggested by theory at a point that data are consistent with no trend at all.

Therefore, data at cosmological redshifts and the tightness of the colour–magnitude relation at low redshift strongly argue against a scenario where many blue galaxies transform themselves in faint red galaxies, whereas the presence of some spiral galaxies on the red sequence in nearby clusters suggests a redshift trend in the relative abundance of faint red galaxies should be observed in sufficiently large cluster samples, although none is clearly revealed in the present one.

### 4.4 Some advantages and shortcomings of present studies

Other authors argue that  $L/F$  or its reciprocal,  $F/L$ , are preferable to  $\alpha$  in the study of the relative abundance of faint red galaxies, usually with the rationale that the Schechter function might not describe the LF in the studied mag range. Beside the fact that the very same authors find acceptable fit on their data (typically,  $\chi^2_v \approx 1$  values), and thus they argue something not supported by their own data, we note that  $L/F$ , and its reciprocal,  $F/L$ , both are quantities difficult to manage from a statistical point of view. For example an average value, computed by a weighted sum, or a fit performed minimizing the  $\chi^2$ , has a special meaning, because the result depends on whether  $L/F$  or  $F/L$  is averaged (fitted). For example, let’s consider two, for sake of clarity, data points,  $(f/l)_1 = 3 \pm 0.9$  and  $(f/l)_2 = 0.3333 \pm 0.1$  and two possible averages. The error weighted average  $\langle f/l \rangle$  is 0.37. The error weighted average  $\langle l/f \rangle$  of the reciprocal values  $(\langle l/f \rangle = 1/\langle f/l \rangle; 0.3333 \pm 0.1$  and  $3 \pm 0.9$ ) is again 0.37, fairly different from the reciprocal of  $\langle f/l \rangle$ ,  $1/0.37 = 2.7$ . Therefore,  $\langle f/l \rangle \neq 1/\langle l/f \rangle$ . At first sight, by choosing the parametrization of

the aimed quantity, the astronomer may chose the result he want. Furthermore,  $\langle f/l \rangle$  has a value near to the point with index 2,  $(f/l)_2$ , whereas  $\langle l/f \rangle$  has a value near to the other data point, with index 1,  $(f/l)_1$ , a strange situation, indeed. Similar problems are present with two data points differing by just  $1 \sigma$ , or with small samples. Therefore, astronomers who want to use  $LIF$  or  $FLI$  are invited first to understand what is going on in the simple case of just two measurements and a fit with a constant (the mentioned weighted average), and then proceed to the case they are really interested in: a few data points and a fit with one more degree of freedom (the redshift or mass dependence).

As mentioned, there are presently a few determinations of the evolution of faint red galaxies. Some of them make different claims concerning the deficit of faint red galaxies at high redshift, yet we have verified that often, but not always, data agree with each other, as shown in Figs 4 and 5, in the (usually small) range where they are well determined. This work offers some advantages with respect to previous ones.

(i) Our determination is more sensitive to evolution, because our cluster sample displays the widest redshift coverage while keeping a large sample of clusters.

(ii) This work minimizes systematics, for example using a colour index bracketing the 4000-Å break at every redshift. Fig. 1 shows that SDSS  $u$  and  $g$  filters and, at a lower extent,  $B$  and  $I$  filters at  $z = 0.25$ , sample the 4000-Å break in similar way as  $HST$  filters do at higher redshift. This is not the rule: for example, De Lucia et al. (2007) use rest-frame  $U - V$  at high redshift but  $r' - i'$  at  $z = 0$  for C4 clusters ( $r'$  and  $i'$  have effective  $\lambda = 6165$  and  $7481 \text{ \AA}$ , respectively). The central wavelength of the bluest filter ( $R$ ) used in the recent  $0.35 < z < 0.95$  study by Gilbank et al. (2008) lies longwards of the Balmer break for  $z < 0.75$  (Fig. 8). By using the same filter pair ( $R - z'$ ) at all redshifts, rather than a color selection mimicking  $U - V$  at all redshifts, their technique introduces a potential bias, as several spiral types move from red to blue between the low and the high redshift samples because of their observational strategy. Furthermore, at  $z \gtrsim 0.55$  the data used by Gilbank et al. (2008) are not deep enough to sample faint galaxies ( $M_V = -18.2 \text{ mag}$ , such as those considered here, in Stott et al. 2007; de Lucia et al. 2007, in Gilbank & Balogh 2008, etc.), see the top panel of Fig. 8. In their later work, Gilbank & Balogh (2008) use data lacking appropriate Balmer break coverage (the  $z = 0.25$  point from Hanson et al. 2008 and the  $z = 0$  point from De Lucia 2007) and omit data with better 4000-Å sampling (Fig. 1) and appropriate depth (those in this work). In passing, we also disagree with their statement about the number of clusters at low redshift in our sample: their claim that it 'only contains two  $z < 0.5$  clusters', while instead our sample includes 12 clusters, 10 from Smail et al. (1998) and two from our own analysis of SDSS data.

(iii) Interlopers are removed using observations taken in the very same bands as cluster observations (see Table 1), to avoid systematics (see Smail et al. 1998; Andreon 2006a). This is often not the case: for cluster and control field Stott et al. (2007) use different filters, whereas De Lucia et al. (2007) use different telescopes and filters. The impact of these systematics is not quantified in the mentioned works.

(iv) We feel our statistical analysis to be preferable: beside already mentioned statistical considerations, there are a number of debatable issues in other works, such as averages of incompatible measurements, Poisson errors for binomial distributed quantities, and unphysical results such as negative number of galaxies.

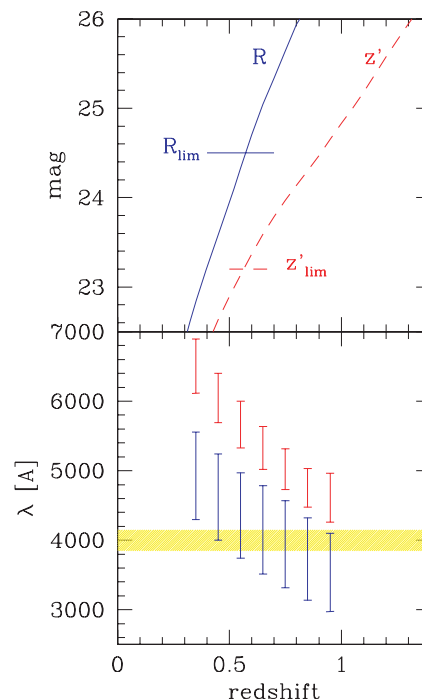


**Figure 8.** Bottom panel: rest-frame  $\lambda$  sampling of the filters used in Gilbank et al. (2008). The shaded (yellow) band marks the 4000-Å break. The central wavelength of the bluest filter ( $R$ ) lies longwards of the Balmer break for  $z < 0.75$  (contrast it to the one in the present work, shown in Fig. 1). Upper panel:  $R$  and  $z'$  mag of a passive evolving  $M_V = -18.2 \text{ mag}$  galaxy (red dashed and blue solid curves, respectively) and the limiting magnitude of the observational material used by Gilbank et al. (2008). Gilbank et al. (2008) data are not deep enough to detect these faint galaxies at  $z \gtrsim 0.55$ .

(v) Our clusters are spectroscopically confirmed and have an X-ray emission that confirms the existence of deep potential wells. Instead, we ignore whether candidate, or putative, clusters without a spectroscopic confirmation or an X-ray detection, studied in some other papers (e.g. Kodama et al. 2004) are clusters or line of sight superpositions. Sometimes, follow-up spectroscopic observations show that a considerable fraction of them are line-of-sight superpositions (e.g. Yamada et al. 2005).

## 5 SUMMARY AND CONCLUSIONS

The history of mass assembly of bright (massive) red galaxies in clusters is pretty well known: they were assembled at early times, as testified by the passive evolution of their characteristic magnitude (e.g. De Propris et al. 1998, 2007; Andreon et al. 2008b), the constancy of their stellar mass function (e.g. Andreon 2006b) and of the halo occupation number, that is, the number of galaxies per unit cluster mass (Lin et al. 2006; Andreon et al. 2008a). We stress that all mentioned works favour the above scenario, but only one, (Andreon 2006b), excludes contender models, and we emphasize that most mentioned works have samples that are dominated, but not exclusively composed, by red galaxies.

The history of mass assembly of faint red galaxies is far less clear. This paper shows that a non-evolution of the faint end slope  $\alpha$ , or any related number such as the luminous-to-faint ratio, is fully compatible with the data. This implies that the history of mass assembly of faint red galaxies is strictly parallel to the one of their

massive cousins, in order to keep the relative abundance constant. Therefore, the build-up of the red sequence is largely complete by  $z = 1.3$  down to  $0.05 L^*$ , and, if a differential filling is envisaged, it should occur mostly at much larger redshift. Similarly, cluster mass, as parametrized by X-ray luminosity or velocity dispersion, seems not to play any role in shaping the relative abundance of faint galaxies, contrary to some previous claims. Our claims are based on one of the largest samples, spread over the wider redshift range studied thus far with a large cluster sample, with great attention to systematics. A recent ( $z < 1.3$ ) transformation of many blue galaxies in faint red galaxies would modify the faint-end slope of the LF, change the  $F/L$  ratio and inflate the color scatter of the colour–magnitude relation, none of which have been observed. Yet, a redshift trend is expected because of the spiral morphology of some faint red galaxies in nearby clusters, but a larger sample of clusters (at  $z \gg 0.5$ ) is needed to measure its small amplitude. The present sample is, however, large enough to discard the claimed steep trends previously suggested in the literature.

## ACKNOWLEDGMENTS

I acknowledge the referee for helping me to improve the presentation of this work, Roberto De Propris, Yusei Koyama, Masayuki Tanaka, Tommaso Treu for useful comments on this draft, Gabriella De Lucia for clarifications about her results and Kevin Pimblet, Nelson Caldwell and Duncan Forbes for helping me with recovering the Tarlevich et al. (2001) Coma catalogue published electronically in MNRAS, but not available on the journal site.

For the standard SDSS acknowledgment see: <http://www.sdss.org/dr5/coverage/credits.html>.

We thank HST programmes 9290, 9919, 9033, 9722, 9498 9744, 9425 and 9583.

## REFERENCES

- Adelman-McCarthy J. K. et al., 2007, *ApJ*, 172, 634  
 Andreon S., 1996, *A&A*, 314, 763  
 Andreon S., 2003, *A&A*, 409, 37  
 Andreon S., 2006a, *MNRAS*, 369, 969  
 Andreon S., 2006b, *A&A*, 448, 447  
 Andreon S., Willis J., Quintana H., Valtchanov I., Pierre M., Pacaud F., 2004, *MNRAS*, 353, 353  
 Andreon S., Cuillandre J.-C., Puddu E., Mellier Y., 2006, *MNRAS*, 372, 60  
 Andreon S., de Propris R., Puddu E., Giordano L., Quintana H., 2008a, *MNRAS*, 383, 102  
 Andreon S., et al., 2008b, *MNRAS*, 385, 979  
 Ball N. M., Loveday J., Brunner R. J., Baldry I. K., Brinkmann J., 2006, *MNRAS*, 373, 845  
 Balogh M. L., Baldry I. K., Nichol R., Miller C., Bower R., Glazebrook K., 2004, *ApJ*, 615, L101  
 Benítez N. et al., 2004, *ApJS*, 150, 1  
 Bertin E., Arnouts S., 1996, *A&AS*, 117, 393  
 Binggeli B., Sandage A., Tammann G. A., 1988, *ARA&A*, 26, 509  
 Bower R. G., Lucey J. R., Ellis R. S., 1992, *MNRAS*, 254, 601  
 Bruzual G., Charlot S., 2003, *MNRAS*, 344, 1000  
 Butcher H., Oemler A., 1984, *ApJ*, 285, 426  
 Cool R. J., Eisenstein D. J., Johnston D., Scranton R., Brinkmann J., Schneider D. P., Zehavi I., 2006, *AJ*, 131, 736  
 D’Agostini G., 2003, *Bayesian Reasoning in Data Analysis: A Critical Introduction*. World Scientific, Singapore  
 D’Agostini G., 2005, preprint (physics/0511182)  
 De Lucia G. et al., 2007, *MNRAS*, 374, 809  
 De Propris R., Eisenhardt P. R., Stanford S. A., Dickinson M., 1998, *ApJ*, 503, L45  
 De Propris R., Stanford S. A., Eisenhardt P. R., Holden B. P., Rosati P., 2007, *AJ*, 133, 2209  
 Ebeling H., Barrett E., Donovan D., Ma C.-J., Edge A. C., van Speybroeck L., 2007, *ApJ*, 661, L33  
 Eisenhardt P. R., De Propris R., Gonzalez A. H., Stanford S. A., Wang M., Dickinson M., 2007, *ApJS*, 169, 225  
 Ettori S., Tozzi P., Borgani S., Rosati P., 2004, *A&A*, 417, 13  
 Ford H. C. et al., 1998, in Bely P. Y., Breckinridge J. B., eds, *Proc. SPIE Vol. 3356, Space Telescopes and Instruments V*. SPIE, Bellingham, p. 234  
 Ford H. C. et al., 2003, in Blades J. C., Siegmund O. H. W., eds, *Proc. SPIE Vol. 4854, Future EUV/UV and Visible Space Astrophysics Missions and Instrumentation*. SPIE, Bellingham, p. 81  
 Gal R. R., Lubin L. M., 2004, *ApJ*, 607, L1  
 Garilli B., Maccagni D., Andreon S., 1999, *A&A*, 342, 408  
 Gilbank D. G., Balogh M. L., 2008, *MNRAS*, 385, L116  
 Gilbank D. G., Yee H. K. C., Ellingson E., Gladders M. D., Loh Y.-S., Barrientos L. F., Barkhouse W. A., 2008, *ApJ*, 673, 742  
 Hack W., 1999, *CALACS Operation and Implementation, Instrument Science Report ACS 99-03*. STScI, Baltimore  
 Hansen S. M., Sheldon E. S., Wechsler R. H., Koester B. P., 2008, *ApJ*, submitted (arXiv:0710.3780)  
 Hogg D. W. et al., 2004, *ApJ*, 601, L29  
 Jorgensen I., Franx M., Kjaergaard P., 1996, *MNRAS*, 280, 167  
 Kodama T. et al., 2004, *MNRAS*, 350, 1005  
 Kodama T., Arimoto N., Barger A. J., Arag’on-Salamanca A., 1998, *A&A*, 334, 99  
 Koekemoer A. M., Fruchter A. S., Hook R. N., Hack W., 2002, in *The 2002 HST Calibration Workshop: Hubble after the Installation of the ACS and the NICMOS Cooling System*. STScI, Baltimore, p. 337  
 Koyama Y., Kodama T., Tanaka M., Shimasaku K., Okamura S., 2007, *MNRAS*, 382, 1719  
 Lin Y.-T., Mohr J. J., Gonzalez A. H., Stanford S. A., 2006, *ApJ*, 650, L99  
 Lubin L. M., Mulchaey J. S., Postman M., 2004, *ApJ*, 601, L9  
 Maughan B. J., Jones L. R., Ebeling H., Scharf C., 2004, *MNRAS*, 351, 1193  
 Oemler A., Jr., 1992, in Fabian A. C., ed., *Clusters and Superclusters of Galaxies*. Kluwer, Dordrecht, p. 29  
 Pahre M. A., de Carvalho R. R., Djorgovski S. G., 1998, *AJ*, 116, 1606  
 Pimblet K. A., Smail I., Kodama T., Couch W. J., Edge A. C., Zabludoff A. I., O’Hely E., 2002, *MNRAS*, 331, 333  
 Schechter P., 1976, *ApJ*, 203, 297  
 Schwarz G., 1978, *Ann. Stat.*, 5, 461  
 Sivia D., 2006, *Data Analysis: A Bayesian Tutorial*. Oxford Univ. Press, Oxford  
 Smail I., Edge A. C., Ellis R. S., Blandford R. D., 1998, *MNRAS*, 293, 124  
 Stanford S. A., Eisenhardt P. R., Dickinson M., 1998, *ApJ*, 492, 461  
 Stanford S. A., Holden B., Rosati P., Tozzi P., Borgani S., Eisenhardt P. R., Spinrad H., 2001, *ApJ*, 552, 504  
 Stott J. P., Smail I., Edge A. C., Ebeling H., Smith G. P., Kneib J.-P., Pimblet K. A., 2007, *ApJ*, 661, 95  
 Terlevich A. I., Caldwell N., Bower R. G., 2001, *MNRAS*, 326, 1547  
 van Dokkum P. G., van der Marel R. P., 2007, *ApJ*, 655, 30  
 Yamada T. et al., 2005, *ApJ*, 634, 861

This paper has been typeset from a  $\text{\TeX}/\text{\LaTeX}$  file prepared by the author.